On Preamble Detection in Packet-Based Wireless Networks

Sumeeth Nagaraj, Sheehan Khan and Christian Schlegel
Department of Electrical and Computer Engineering
University of Alberta,
Edmonton, Canada.
Email:{snagaraj,sheehan,schlegel}@ece.ualberta.ca

Marat Burnashev
Institute for Problems of Information Transmission
Bolshoi Karetni 19,
101447, Moscow, RUSSIA.
Email: burn@iitp.ru

***Abstract*— Performance bounds on detecting a preamble embedded at the start of every packet for communication over an additive white Gaussian noise channel are derived. The preamble sequence consists of blocks of spreading sequences whose length is at most the coherence time of the channel. These blocks are differentially combined. A correlation-based detection is employed to locate the boundaries of the preamble. Simulation results closely follow the analysis. Furthermore, the effects of frequency offset on the system performance are discussed.**

I. Introduction

A significant number of present day wireless systems are based on packetized communication. For instance, the IEEE standards for local, metropolitan and personal area networks, and several cellular communication standards. In such communication systems, packet arrival instants are generally random and unknown at the receiver. The payload can be successfully demodulated provided the receiver has *symbol timing*, *frequency* and *phase offset* information, in addition to achieving *frame synchronization*. In many practical applications, these parameters are not known a priori at the receiver and hence have to be estimated from the received signal.

To facilitate the process of synchronization, a preamble is prefixed for each payload transmission. Additionally, a synchronization (sync) pattern included in the preamble enables frame synchronization. Figure 1(a) shows a typical packet format with preamble and sync sequence prefixed to the payload, however, the fundamental problem is to achieve frame synchronization, i.e., finding the exact starting time of the payload and a more general view is given in Figure 1(b).

If perfect timing, frequency and phase offset estimates are available at the receiver[1], a typical frame synchronization algorithm correlates the known sync word with the received sequence to find the start of the packet. The maximum correlation peak determines the location of the sync word. On the other hand, without the frequency and phase offset estimates, the baseband signal rotates thereby degrading the performance of a correlation-based preamble detection.

The effect of carrier phase offset can be overcome by using differential encoded phase modulation. This scheme, however, requires nearly 3 dB additional signal-to- noise ratio to achieve the same performance as coherent detection [1]. To mitigate this performance loss, coherent detection is employed on portions (blocks) of the sequence whose length is no longer than the coherence time of the channel [2], [3]. These blocks are then combined differentially.

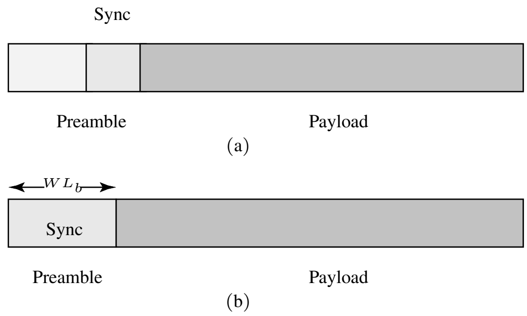

Fig. 1. Packet Formats.

In this paper, we investigate the performance of a new preamble detection method for an uncoordinated direct sequence spread spectrum system (DSSS) using the modified packet format as shown in Fig. 1(b). The preamble is made up of a sequence of W blocks, which are differentially encoded and modulated by a random DSSS sequence of L_b chips per block. A correlation type preamble detector is employed. The analysis assumes a Poisson source traffic model with packet inter-arrival instants modeled by an exponential distribution.

In [4] the preamble detection problem for a TDMA system employing coherent detection was considered. Note that coherent preamble detection requires frequency and phase offset estimates and hence the system incurs rate loss. Moreover, in a TDMA system, packet arrival instants are known at the receiver to be at the beginning of each time slot. Hence, a preamble is either detected or missed. However, in an uncoordinated multiple access system the packet arrival instants are random. This leads to an additional event of erroneously detecting a preamble.

The rest of the paper is organized as follows. In Section II we describe the system model and the preamble detection algorithm. Based on the proposed system model, performance bounds on the preamble detection algorithm are derived in Section III. In Section IV, simulation results are provided to

[1]Estimation of frequency and phase offset require pilot signal. Hence the system incurs rate loss.

show the accuracy of the analysis. The conclusions follow in Section V.

II. System Model and Assumptions

The packet arrival pattern is modeled as a Poisson process with intensity λ. The packet inter-arrival instants follow a truncated exponential distribution in the time window $[1, S]$. Therefore, the packet inter-arrival time distribution is given by

$$p_{i_0}(i) = \begin{cases} c(S)\lambda e^{(-\lambda i)}, & 1 \le i \le S \\ 0, & \text{otherwise} \end{cases} \quad (1)$$

where $c(S)$ is a normalization constant

$$c(S) = \frac{1}{\sum_{i=1}^{S} \lambda e^{-\lambda i}} = \frac{1 - e^{-\lambda}}{\lambda e^{-\lambda}(1 - e^{-S\lambda})}. \quad (2)$$

The modulator block diagram is shown in Figure 2. The preamble sequence $\mathbf{c} = (c_0, c_1, \ldots, c_{W-1})$ composed of independent and identically distributed binary phase shift keying (BPSK) bits, i.e., $c_m \in \{1, -1\}$, is differentially encoded into a sequence $\{a_m\}$, wherein $a_m = c_m a_{m-1}$ with initial value $a_0 = c_0$. The sequence $\{a_m\}$ is then oversampled by a factor L_b and multiplied by a random but known spreading (chip) sequence $\{b_k\}$ resulting in $\{d_k\}$, for $k = 0 \ldots L_b W - 1$. The block interval is given by $T_b = L_b T_c$, where T_c is the chip interval. The spreading sequence $\{b_k\}$ consists of independent and identically distributed random variables with $\mathrm{P}(b_k = 1) = P(b_k = -1) = 1/2$. The spreading sequence need not be periodic but periodic sequences lead to significantly less complex hardware implementations. The complex envelope of the transmitted signal $s(t)$ has the form

$$s(t) = \sqrt{E_c} \sum_{k=0}^{L_b W - 1} d_k p(t - kT_c - i_0 T_c), \quad (3)$$

where $i_0 \in [1, S]$ is the starting moment of the preamble, E_c denotes energy per chip and $p(t)$ is a pulse shaping function with support $[0, T_c]$ and normalized to unit energy.

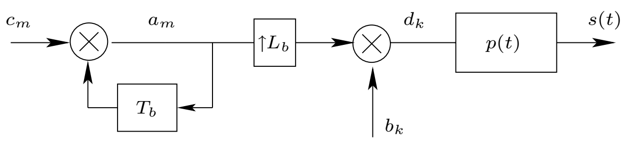

Fig. 2. Modulator block diagram

We consider communication over an additive white Gaussian noise (AWGN) channel. The received signal is represented as

$$r(t) = e^{(2\pi\Delta f t + \phi)j} s(t) + \mathbf{n}(t), \quad (4)$$

where Δf and ϕ denotes carrier frequency and phase offset respectively. The frequency offset is a constant whereas phase offset is modeled as a uniform random variable in the interval $[0, 2\pi)$. Additionally, the transmitted signal $s(t)$ is corrupted by $\mathbf{n}(t)$, a zero mean complex valued Gaussian white noise process with independent real and imaginary components each with variance $N_0/2$.

Assuming perfect chip timing knowledge at the receiver[2] and after chip-matched filtering and sampling, the baseband output is represented as

$$r(k) = s(k) e^{j(2\pi\Delta f T_c k + \phi)} + \mathbf{n}(k). \quad (5)$$

These samples are despread and summed to obtain $\hat{a}_m$, a complex valued estimate of the bit a_m, i.e.,

$$\hat{a}_m(k) = \sum_{l=mL_b}^{(m+1)(L_b-1)} r(l+k) b_l \quad \text{for } m = 0 \ldots W-1. \quad (6)$$

To detect the boundaries of the preamble we use the following decision rule. The receiver differentially correlates the sequence $\{\hat{a}_m(k)\}$ with the known preamble. The correlation threshold at kth time interval is given by

$$\eta_k = \frac{1}{L_b} \sum_{m=0}^{W-1} \hat{a}_m(k) \hat{a}_{m-1}^*(k) c_m, \quad (7)$$

where $\hat{a}^*$ denotes the complex conjugate of $\hat{a}$ and η_k is a complex decision variable. The preamble detection algorithm computes η_k at every chip time interval. Note that only the real part of the decision variable η_k is required to make a decision. The decision variable $\mathbf{Re}\ \eta_k$ greater than a threshold G indicates the presence of a preamble, i.e., at the stopping moment: $\min\{k \in [1, S] : \mathbf{Re}\ \eta_k \ge G\}$.

The threshold G is the correlation peak for a perfect overlap case with $k = i_0$ for the noise free case. This is defined as

$$G \stackrel{\text{def}}{=} (1 - g)(W - 1) L_b E_c \cos(2\pi\Delta f L_b T_c), \quad (8)$$

where $g \in [0, 1]$ determines a fraction of the threshold level G.

III. Performance Analysis

We define two error events conditioned on the presence of the preamble at moment i_0. First, the decision variable being greater than the threshold G, at moment $k < i_0$, flags the erroneous presence of a preamble. We call such an event a *wrong detection* and denote its probability by $\mathrm{P}(\text{wrong}|i_0)$. Secondly, a preamble is missed if the decision variable at moment i_0, is less than the threshold G. We call such an event a *miss* and denote its probability by P(miss). The probability of successful preamble detection is then given by

$$\mathrm{P(success)} = 1 - \mathrm{P(wrong)} - \mathrm{P(miss)}. \quad (9)$$

A. Probability of Missing a Preamble

Assuming that a preamble starts at i_0, the probability of missing the preamble is given by

$$\mathrm{P(miss)} = \mathrm{P}(\mathbf{Re}\ \eta_{i_0} \le G). \quad (10)$$

[2]This assumption leads to an upper bound on the performance of the preamble detection method for an asynchronous system.

The decision variable $\mathbf{Re}\ \eta_{i_0}$ may be expressed in the quadratic form

$$\begin{aligned}\mathbf{Re}\ \eta_{i_0} &= \frac{1}{2}\sum_{m=0}^{W-1} c_m \left(\hat{a}_m(i_0)\hat{a}^*_{m-1}(i_0) + \hat{a}^*_m(i_0)\hat{a}_{m-1}(i_0)\right) \\ &= \frac{1}{2}\hat{\mathbf{a}}^\dagger \mathbf{C}\hat{\mathbf{a}}, \end{aligned} \tag{11}$$

where $[\cdot]^\dagger$ denotes conjugate transpose, and $\hat{\mathbf{a}} = (\hat{a}_0, \hat{a}_2, \ldots, \hat{a}_{W-1})^T$. Further, the estimates $\{\hat{a}_m\}$ are complex Gaussian random variables with expectation $\boldsymbol{\mu}_a$. The $(W \times W)$ matrix $\mathbf{C}$ is symmetric with entries,

$$\mathbf{C}_{\min(i,j)} = \begin{cases} c_{i+1}, & |i-j| = 1 \\ 0, & \text{otherwise.} \end{cases} \tag{12}$$

Note that the entries in the vector $\hat{\mathbf{a}}$ are not independent because of differential encoding. In general, to make the entries independent we first apply a whitening transformation. The uncorrelated vector is then orthogonally rotated to obtain independent components. In this problem, the variance-covariance matrix is the identity matrix, i.e.,

$$\boldsymbol{\Sigma}_{\boldsymbol{a}} = \mathrm{E}(\hat{\boldsymbol{a}} - \boldsymbol{\mu}_a)(\hat{\boldsymbol{a}} - \boldsymbol{\mu}_a)^\dagger = \mathbf{I}. \tag{13}$$

where $N_0 = 1$. Furthermore, there exists a matrix $\mathbf{P}$ such that

$$\mathbf{P}^T\mathbf{C}\mathbf{P} = \boldsymbol{\Lambda},\ \mathbf{P}^T\mathbf{P} = \mathbf{I}, \tag{14}$$

where $\boldsymbol{\Lambda}$ is the diagonal Eigenvalue matrix of $\mathbf{C}$. Now, substituting for $\mathbf{C}$ in (11) results in

$$\mathbf{Re}\ \eta_{i_0} = \frac{1}{2}\hat{\mathbf{a}}^\dagger \mathbf{P}\boldsymbol{\Lambda}\mathbf{P}^T\hat{\mathbf{a}} = \frac{1}{2}\mathbf{Z}^\dagger\boldsymbol{\Lambda}\mathbf{Z} = \frac{1}{2}\sum_{i=0}^{W-1}\lambda_i |Z_i|^2, \tag{15}$$

where $\mathbf{Z} = \mathbf{P}^T\hat{\mathbf{a}}$, is an independent complex Gaussian vector with unit variance and expected value $\mathrm{E}[\mathbf{Z}] = \mathbf{P}^T\boldsymbol{\mu}_a$. Therefore, $|Z_i|^2$ are non central chi-squared distributed random variables with two degrees of freedom and non-centrality parameter given by $\delta_i^2 = |\mathrm{E}[Z_i]|^2$. Hence the quadratic form is a linear combination of non central chi-square distributed random variables.

In the sequel the following Lemma will be needed.

Lemma 1: The Eigenvalues λ_i and corresponding Eigenvectors $\mathbf{p}_i$ of the matrix $\mathbf{C}$ are given by

$$\begin{aligned}\lambda_i &= -2\cos\left(\frac{\pi i}{W+1}\right),\ 1 \le i \le W. \\ p_{ij} &= -2\prod_{k=1}^{j-1} c_k \cot\left(\frac{i\pi}{W+1}\right)\sin\left(j\left(\pi - \frac{i\pi}{W+1}\right)\right), \\ &\quad 1 \le i, j \le W,\end{aligned}$$

where $\lambda_1 < \lambda_2 < \ldots < \lambda_W$.

Proof: See [5] ∎

The probability of miss (10) is given by,

$$\mathrm{P(miss)} = \mathrm{P}(\mathbf{Re}\ \eta_{i_0} < G) = \mathrm{P}\left(\sum_{i=0}^{W-1}\lambda_i|Z_i|^2 < 2G\right). \tag{16}$$

The distribution function of a linear combination of noncentral chi-square random variables is calculated using the characteristic function (c.f) approach and numerical integration (see Appendix). The distribution function can also be evaluated by a series expansion given in [6]. However, the rate of convergence becomes slower for increasing values of W.

B. Probability of Erroneous Detection

The probability of wrong detection conditioned on the occurrence of the preamble at moment i_0 is given by

$$\begin{aligned}\mathrm{P}(\mathrm{wrong}|i_0) &= \mathrm{P}\left(\bigcup_{k=1}^{i_0-1}\mathbf{Re}\ \eta_k \ge G|i_0\right) \\ &\le \sum_{k=1}^{i_0-1}\mathrm{P}(\mathbf{Re}\ \eta_k \ge G|i_0).\end{aligned} \tag{17}$$

The inequality in (17) is obtained by using the union bound on the erroneous detection events. We consider two cases based on the correlation overlap.

$$\begin{aligned}\mathrm{P}(\mathrm{wrong}|i_0) &\le \sum_{k=1}^{(i_0-WL_b)_+}\mathrm{P}(\mathbf{Re}\ \eta_k \ge G|i_0) \\ &+ \sum_{k=(i_0-WL_b+1)_+}^{i_0-1}\mathrm{P}(\mathbf{Re}\ \eta_k \ge G|i_0)\end{aligned} \tag{18}$$

Assuming that $i_0 - WL_b \ge 1$, the first case involves correlating the known preamble with the received Gaussian noise samples. The second case captures partial correlation of the known preamble sequence with the received preamble.

Case 1. $1 \le k \le i_0 - WL_b$**:** The decision variable, η_k, may be written in the quadratic form

$$\mathbf{Re}\ \eta_k = \frac{1}{2}\hat{\mathbf{a}}^\dagger\mathbf{C}\hat{\mathbf{a}}, \tag{19}$$

where $\hat{\mathbf{a}}^T = [\mathbf{n}(k), \mathbf{n}(k+1), \ldots, \mathbf{n}(k+W-1)]$. After mean removal, whitening and orthogonal transformation, (19) may be written as

$$\mathbf{Re}\ \eta_k = \frac{1}{2}\mathbf{Z}^\dagger\boldsymbol{\Lambda}\mathbf{Z} = \frac{1}{2}\sum_{i=k}^{k+W-1}|Z|_i^2\lambda_i, \tag{20}$$

where $\mathbf{Z} = \mathbf{P}^T\hat{\mathbf{a}}$ is a complex standard Gaussian random vector. Therefore, $|Z|_i^2$ are central chi-square distributed random variables with two degrees of freedom. Equation (20) is a linear combination of central chi-squared distributed random variables. The distribution function of a linear combination of central chi-squared distributed random variables can be computed in closed form (see Appendix). Therefore,

$$\begin{aligned}&\sum_{k=1}^{(i_0-WL_b)_+}\mathrm{P}\ (\mathbf{Re}\ \eta_k \ge G|i_0) \\ &= (i_0 - WL_b)_+\mathrm{P}\left(\sum_{i=0}^{W-1}|Z|_i^2\lambda_i \ge 2G|i_0\right) \\ &= (i_0 - WL_b)_+\sum_{r=1}^{W}\left(\prod_{i=1,i\ne r}^{W}\frac{1}{\lambda_r - \lambda_i}\right)\frac{e^{-G/(\lambda_r)}}{\lambda_r},\end{aligned}$$

where the W Eigenvalues λ_i's of the matrix $\mathbf{C}$ are computed using Lemma 1.

Case 2. $i_0 - WL_b + 1 \leq k \leq i_0 - 1$**:** The decision variable may be written in the same form as in (20). Note that, unlike in the previous case, $\mathbf{Z} = \mathbf{P}^T\hat{\mathbf{a}}$, is an independent complex Gaussian vector with unit variance and expected value $\mathrm{E}[\mathbf{Z}] = \mathbf{P}^T\boldsymbol{\mu}_a$. Therefore, $|Z_i|^2$'s are non central chi-square distributed random variables with two degrees of freedom and non-centrality parameters given by $\delta_i^2 = |\mathrm{E}[Z_i]|^2$, $(i = 0 \ldots W-1)$. The required probabilities, i.e., $\mathrm{P}(\mathbf{Re}\ \eta_k \geq G|i_0)$, for $i_0 - WL_b + 1 \leq k \leq i_0 - 1$ are calculated from the characteristic function approach and numerical integration (see Appendix).

Using the above two cases in (18) we obtain an upper bound on $\mathrm{P}(\text{wrong}|i_0)$. The probability of wrong detection is then given by the formula of total probability as

$$\begin{aligned}
\mathrm{P}(\text{wrong}) &= \sum_{i=1}^{S} \mathrm{P}(\text{wrong}|i)\mathrm{P}(i_0 = i) && (21)\\
&\leq \sum_{i=1}^{S}\sum_{k=1}^{i-1} \mathrm{P}(\mathbf{Re}\ \eta_k \geq G|i)\mathrm{P}(i_0 = i) && (22)\\
&\approx (\frac{1}{\lambda} - 1)\mathrm{P}(\mathbf{Re}\ \eta_1 \geq G), && (23)
\end{aligned}$$

where the factor $1/\lambda - 1$ accounts for the traffic intensity and approximation in (23) is permissible if $E_c \ll N_0$ where the self-noise is negligible. Further, the probability in (23) is evaluated for Case 1.

A lower bound on the probability of successful detection P(success) is obtained by substituting (21) and (16) in (9).

IV. Analytical and Simulation Results

The performance of the proposed preamble detection algorithm is evaluated in terms of probability of miss and probability of erroneously detecting a packet versus signal to noise ratio.

The probability of packet miss is shown in Figure 3 for different SNR and frequency offset values. Here, we consider a preamble sequence of length $W = 30$ bits. These bits are differentially encoded and then multiplied by a pseudo noise code of spreading factor $L_b = 32$. The threshold level g is set to 0.5 and (16) is used to plot the probability of miss. From Figure 3 we can observe that the simulation results closely follow the analysis. Further, note that a frequency offsets, $\Delta f = 0.1/(32T_c)$ and $\Delta f = 0.2/(32T_c)$, results in performance degradation of 0.7dB and 4.1 dB respectively. This is because, presence of frequency offset rotates the signal and degrades the system performance. To compensate for the performance degradation, the block length L_b is made at most equal to the coherence time of the channel.

Figure 4 shows an upper bound on the probability of erroneous detection (18) (17) for different SNR (E_c/N_0) and frequency offset values. From this figure, we can observe a good agreement between the analysis and simulation results. Further, the performance degradation due to frequency offset is shown. At low E_c/N_0 values, an approximation for the probability of erroneous detection given in (23) matches closely with the upper bound.

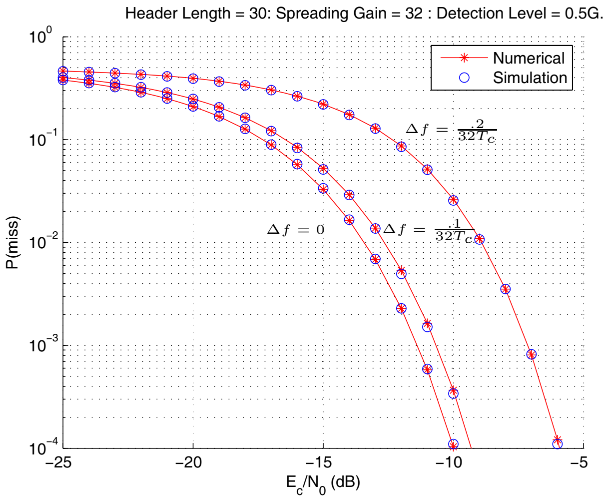

Fig. 3. Probability of missing a packet for the proposed preamble detection algorithm is shown for different SNR and frequency offset values.

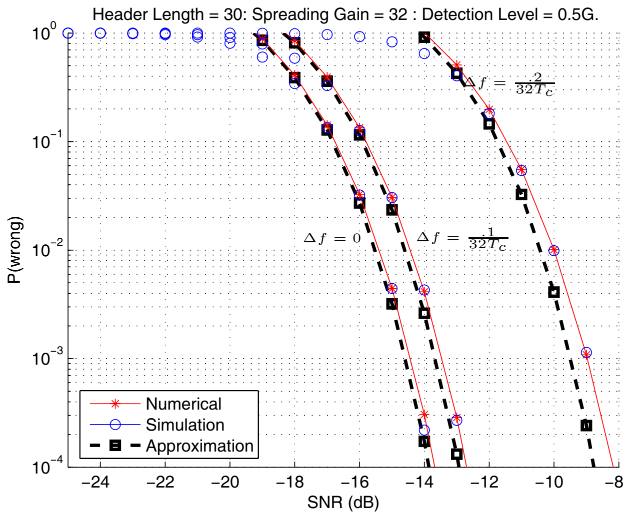

Fig. 4. Probability of erroneous packet detection for the proposed preamble detection algorithm is shown for different SNR and frequency offset values without using the traffic intensity factor.

The receiver operating curves are given in Figure 5 for different detection threshold values. It can be seen from the figure that as the detection threshold is lowered (increasing g) the probability of miss decreases while probability of false alarm increases. On the other hand, increasing the detection threshold (decreasing g) leads to lower false alarms but higher probability of missing a packet.

V. Conclusion

We derived performance bounds on detecting a preamble sequence embedded at the start of each packet transmission over an AWGN channel. Exact results were provided for the

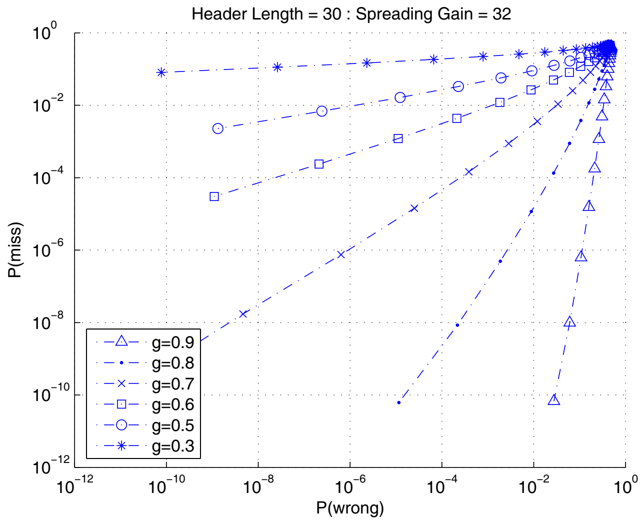

Fig. 5. Receiver operating curves is shown for different detection threshold levels. SNR values $E_c/N_0 \in [-23, -5]$dB are plotted at 1 dB interval.

probability of missing a packet. Further, an upper bound on the probability of erroneous detection closely matches with the simulation results. Due to block differential encoding, the proposed preamble detection method does not require phase offset estimates. However, it is shown that for frequency offsets $\Delta f = 0.1/(32T_c)$ and $\Delta f = 0.2/(32T_c)$, the system requires 0.7 dB and 4.1 dB additional E_c/N_0 over the zero frequency offset case to achieve a P(miss) $= 10^{-4}$. The performance loss is somewhat significant for P(wrong). Additionally, an approximation for the probability of erroneous detection is provided for low E_c/N_0 values; the approximation closely follows with the upper bound results.

Appendix

Distribution function of a linear combination of non-central chi-square random variables. Let $Z_i \sim \mathcal{CN}(\mu_i, 1)$. The characteristic function of the random variable $\lambda_i|Z_i|^2$ is given by

$$\Phi_i(t) = \mathrm{E}\left[\exp\left(jt\lambda_i|Z_i|^2\right)\right] = \frac{\exp\left(j\lambda_i\delta_i t/(1-2j\lambda_i t)\right)}{(1-2j\lambda_i t)} \tag{24}$$

Therefore, the c.f of a linear combination of non central chi-square distributed random variables is

$$\begin{aligned}\Phi(t) &= \mathrm{E}\left[\exp\left(jt\sum_{i=0}^{W-1}\lambda_i|Z_i|^2\right)\right] \\ &= \frac{\exp\left\{jt\sum_{i=0}^{W-1}\lambda_i\delta_i/(1-2jt\lambda_i)\right\}}{\prod_{i=0}^{W-1}(1-2jt\lambda_i)}\end{aligned}$$

The distribution function is obtained using Gil-Pelaez's inversion formula [7], [8]

$$\mathrm{F}(x) = \frac{1}{2} + \frac{1}{2\pi}\int_0^\infty \frac{e^{jtx}\Phi(-t) - e^{-jtx}\Phi(t)}{jt}\,\mathrm{d}t \tag{25}$$

The c.f. inversion formula is evaluated numerically using the trapezoidal method to obtain the probabilities.

Distribution function of a linear combination of central chi-Square random variables. Let $Z_i \sim \mathcal{CN}(0,1)$. The characteristic function of the random variable $\lambda_i|Z_i|^2$ is given by

$$\Phi_i(t) = \mathrm{E}\left[\exp\left(jt\lambda_i|Z_i|^2\right)\right] = \frac{1}{(1-2j\lambda_i t)} \tag{26}$$

Therefore, the c.f of a linear combination of central chi-square distributed random variables is

$$\Phi(t) = \prod_{i=1}^{W}\frac{1}{1-2j\lambda_i t}. \tag{27}$$

After partial fraction expansion, (27) is written as [9],

$$\Phi(t) = \sum_{r=1}^{W}\left(\sum_{i=1, i\neq r}^{W}\frac{\lambda_r}{\lambda_r-\lambda_i}\right)\frac{1}{1-2j\lambda_r t}. \tag{28}$$

Now, the probability density function is obtained using the inversion formulae,

$$F'(x) = \sum_{r=1}^{W}\left(\prod_{i=1, i\neq r}^{W}\frac{\lambda_r}{\lambda_r-\lambda_i}\right)\frac{e^{-x/(2\lambda_r)}}{\lambda_r} \tag{29}$$

References

[1] J. Proakis, *Digital Communications*. New York: McGraw-Hill, 2001.
[2] D. Divsalar and M. Simon, "Multiple-symbol differential detection of MPSK," *Communications, IEEE Transactions on*, vol. 38, no. 3, pp. 300–308, March 1990.
[3] G. Colavolpe and R. Raheli, "Improved differential detection of chip-level differentially encoded direct-sequence spread-spectrum signals," *Wireless Communications, IEEE Transactions on*, vol. 1, no. 1, pp. 125–133, Jan. 2002.
[4] M. R. Soleymani and H. Girard, "The effect of the frequency offset on the probability of miss in a packet modem using cfar detection method," *Communications, IEEE Transactions on*, vol. 40, no. 7, pp. 1205 – 1211, Jul. 1992.
[5] S. Nagaraj, S. Khan, C. Schlegel, and M. V. Burnashev, "On preamble detection in packet-based wireless networks," *submitted to Communications, IEEE Transactions on*.
[6] D. Raphaeli, "Distribution of noncentral indefinite quadratic forms in complex normal variables," *IEEE Transactions on Information Theory*, vol. 42, no. 3, pp. 1002–1006, May. 1996.
[7] R. B. Davies, "Numerical inversion of characteristic function," *Biometrika*, vol. 60, no. 2, pp. 415–417, 1973.
[8] J. Gil-Pelaez, "Note on the inversion theorem," *Biometrika*, vol. 38, pp. 481–482, 1951.
[9] C. Schlegel, "Trellis coded modulation on time-selective fading channels," *Communications, IEEE Transactions on*, vol. 42, p. 16171627, April. 1994.